Journal of the Korea Institute of Applied Superconductivity and Cryogenics
Vol.6, No.2, (2004), pp.1~6

Experimental and numerical approaches for AC loss estimation in high T_c superconductors

Naoyuki Amemiya

Yokohama National University

ame@rain.dnj.ynu.ac.jp

Abstract-- **It is important to estimate the total AC loss which is the total energy, or power, dissipated in the superconductor in the simultaneous application of AC transport current and an AC external magnetic field. Experimental and numerical works on AC loss estimation of high Tc superconductors in the author's group are reviewed. The method and the set-up for total AC loss measurements are described. The experimental results for a twisted Bi-2223 multifilamentary tape and a Y-123 film conductor are given. A general theory for numerical electromagnetic field analysis of superconductor by the finite element method is explained. The numerical results for twisted Bi-2223 multifilamentary tapes and a rectangular superconductor simulating coated conductors are presented.**

1. INTRODUCTION

Reduction of AC loss is one of the key issues for power applications of high Tc superconductors, and understanding its characteristics are very important part of R&D activities of high Tc superconductor application. Generally, in AC electrical power devices, high Tc superconductors must carry AC transport current in an AC external magnetic field. Therefore, it is important to estimate the total AC loss which is the total energy, or power, dissipated in the superconductor in this simultaneous application of AC transport current and an AC external magnetic field. There are experimental and theoretical approaches for AC loss estimation. Among theoretical approaches, numerical one is getting popular, because the AC loss in complicated electromagnetic conditions and / or conductor geometries can be estimated.

In this paper, experimental and numerical works on AC loss estimation of high Tc superconductors in the author's group are reviewed. In chapter 2, first, the experimental method and set-up for AC loss measurements are described. Then, experimental results on Bi-2223 multifilamentaty tapes and Y-123 film conductors are presented. In chapter 3, first, numerical model for AC loss analysis using the finite element method is described. Then, numerical results for Bi-2223 multifilamentaty tapes and a rectangular superconductor simulating a coated conductor are presented.

2. EXPERIMENTAL ESTIMATION OF AC LOSS

2.1. Experimental method and set-up for AC loss measurements

2.1.1. Overall system [1]

A schematic view of our set-up for total AC loss measurements is shown in Fig. 1. The whole magnet system and the sample superconductor are cooled in liquid nitrogen. The transverse magnetic field is applied by a dipole magnet. This dipole magnet consists of four racetrack coils to improve the field uniformity in its bore where the sample superconductor is placed. A capacitor bank for compensation of the inductive voltage is connected in series with the magnet to enable the excitation using a variable-frequency bipolar power-supply with a limited output voltage. An AC transport current that is in-phase with the applied transverse magnetic field is supplied to the sample superconductor. This current is supplied by another variable-frequency power-supply through transformers for isolation and current step-up. The sample superconducting tape can be rotated to change the field angle α.

The magnetization loss which is the energy flow from the external magnetic field applied by the magnet is measured using a linked pick-up coil (LPC). The transport loss which is the energy flow from the transport-current

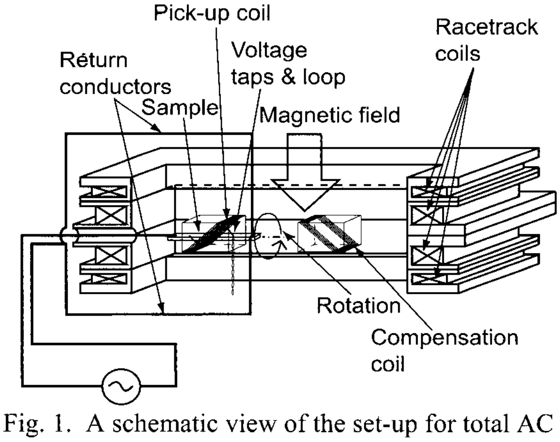

Fig. 1. A schematic view of the set-up for total AC loss measurement in transverse magnetic field.

power supply is measured using voltage taps with a spiral loop.
During the simultaneous application of AC transport current and an AC transverse magnetic field, the magnetization loss & the transport loss are measured separately, and their sum provides us the total AC loss [1]-[3].

The detailed of the transport loss measurements using voltage taps with a spiral loop was provided by other authors [4]. In the following, the magnetization loss measurements using the LPC are described in detail.

2.1.2. Magnetization loss measurements using LPC [1]

A schematic view of the LPC is shown in Fig. 2. The LPC is linked to a sample and is large enough that the sample can be rotated inside it to vary α. In principle, the Poynting vector going into a box enclosed by one turn of the LPC, which equals the loss power dissipated in the sample superconductor within the box, is measured by the LPC. The AC loss energy of the sample per unit volume per cycle, Q_{m}, is

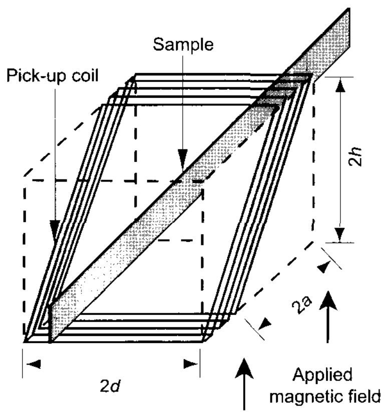

Fig. 2. The linked pick-up coil (LPC).

$$Q_{\mathrm{m}} = -\frac{1}{v_{\mathrm{s}}} \int_T \int_{S_0} (\boldsymbol{E} \times \boldsymbol{H}) \cdot \boldsymbol{n} \mathrm{d}S \mathrm{d}t \,, \tag{1}$$

where T, v_{s}, S_0, $\boldsymbol{n}$, $\boldsymbol{E}$, $\boldsymbol{H}$ are the period, the sample volume in the box, the whole surface of the box, its normal vector, the electric field on the surface of the box, and the magnetic field on the surface of the box, respectively. Here, we assume that $\boldsymbol{H}$ in equation (1) is substituted by the external magnetic field produced by the dipole magnet $\boldsymbol{H}_{\mathrm{e}}$, and then following approximated expression is derived from equation (1).

$$Q_{\mathrm{m}} \approx \frac{2hH_{0,\mathrm{rms}}V_{\mathrm{in,rms}}}{Nfv_{\mathrm{s}}} \,, \tag{2}$$

where $H_{0,\mathrm{rms}}$, $V_{\mathrm{in,rms}}$ and f are the rms of the applied external magnetic field, the rms of the output voltage component of the LPC which is in-phase with the externally applied magnetic field, and the frequency of the magnetic field, respectively. $V_{\mathrm{in,rms}}$ is measured with a lock-in amplifier using the output voltage of a non-inductive shunt resistor as the phase reference. $H_{0,\mathrm{rms}}$ is determined from the magnet current and the magnetic field constant of the magnet. Due to the above mentioned assumption, a calibration factor C must be multiplied to obtain the absolute value of the magnetization loss:

$$Q_{\mathrm{m}} = C\frac{2hH_{0,\mathrm{rms}}V_{\mathrm{in,rms}}}{Nfv_{\mathrm{s}}} \,. \tag{3}$$

The C can be determined by analytical way [1], [5] or experimental way [1], [2]. The cross sectional dimension of the LPC used is 33 mm × 33 mm. This dimension is so large that C is not substantially influenced by a sample width up to 10 mm or sample orientation and can be fixed at 2.0 [1].

Several types of pick-up coils which have been used for the total AC loss measurements are compared in Table I.

TABLE I.
COMPARISON AMONG SEVERAL TYPES OF PICK-UP COIL USED IN TOTAL AC LOSS MEASUREMENTS

	Saddle coil	Flat loop	Race-track or rectangular pick-up coil RTPC	Linked pick-up coil LPC
Schematics	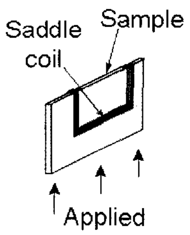	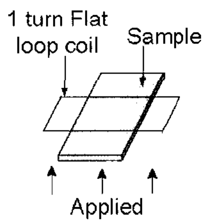	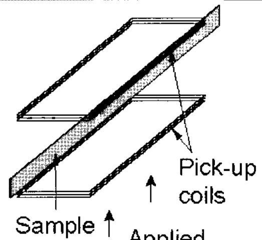	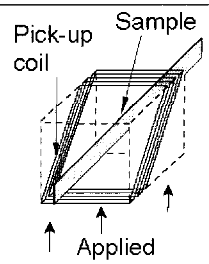
Field direction	Parallel	Perpendicular	Variable	Variable
Angle dependence of sensitivity	N.A.	N.A.	Considerably dependent	Almost independent
Sample insertion and removal	Impossible	Impossible	Possible	Possible

Variable field angle and less angle-dependent sensitivity are advantages of the LPC. A saddle shape pick-up coil which is different from the one in Table I has a same feature, and was used for the magnetization loss measurement without AC transport current [5].

2.2. Experimental results

2.2.1. Total AC loss of Bi-2223 multifilamentary tape [6], [7]

Total AC loss of a Bi-2223 multifilamentary tape whose specifications are listed in Table II was measured using the set-up described in 2.1. This tape was fabricated by KERI in DAPAS program. The frequency of magnetic field and current is 72.44 Hz.

In Figs. 3(a) and 3(b), magnetization loss Q_m, transport loss Q_t, and total AC loss Q_{total} in transverse magnetic fields parallel and perpendicular to the tape wide-face, respectively, are plotted against the amplitude of the transverse magnetic field B_m. Here, the peak of the transport current is about half of the critical current. In a parallel transverse magnetic field, the Q_{total} is dominated by the Q_t in a low field region and is dominated by the Q_m in a high field region. In a perpendicular transverse magnetic field, the Q_{total} is dominated by the Q_m in most of the field range on the measurements.

2.2.2. Total AC loss of Y-123 film conductor [8], [9]

Total AC loss of a Y-123 film conductor whose specifications are listed in Table III was measured using the set-up described in 2.1. This conductor is a commercially available one where Y-123 film is deposited on sapphire substrate by co-evaporation technique. The frequency of magnetic field and current is 72.44 Hz.

In Figs. 4(a) and 4(b), the Q_m, the Q_t, and the Q_{total} in transverse magnetic fields parallel and perpendicular to the tape wide-face, respectively, are plotted against B_m. In a parallel transverse magnetic field, the Q_m is negligible, and the Q_t almost equals the Q_{total}. It is to be noted that the Q_t, hence Q_{total}, increases with increasing B_m. In a perpendicular transverse magnetic field, the Q_{total} is dominated by the Q_m in most of the field range in the measurements.

In Fig. 5, the Q_{total} for $\alpha = 5$ degrees, 45 degrees, and 90 degrees are plotted against $B_m \sin\alpha$. All plots collapse to one curve. The collapsed plots approach to the analytical value of the magnetization loss of superconducting strip without transport current by Brandt and Indenbom with increasing $B_m \sin\alpha$ [10] and approach to the analytical value of the transport loss of superconducting strip without external magnetic field by Norris [11].

TABLE II.
SPECIFICATIONS OF BI-2223 MULTIFILAMENTARY TAPE FOR AC LOSS MEASUREMENTS

Tape width	3.77 mm
Tape thickness	0.24 mm
Cross section of filamentary region	0.58 mm^2
Number of filaments	55
Twist pitch	8.2 mm
Critical current	36.2 A
n value	13.5

3. NUMERICAL ESTIMATION OF AC LOSS

3.1. Numerical model for electromagnetic field analysis of superconductor for AC loss estimation [12, 13]

The AC loss in superconductor can be estimated from

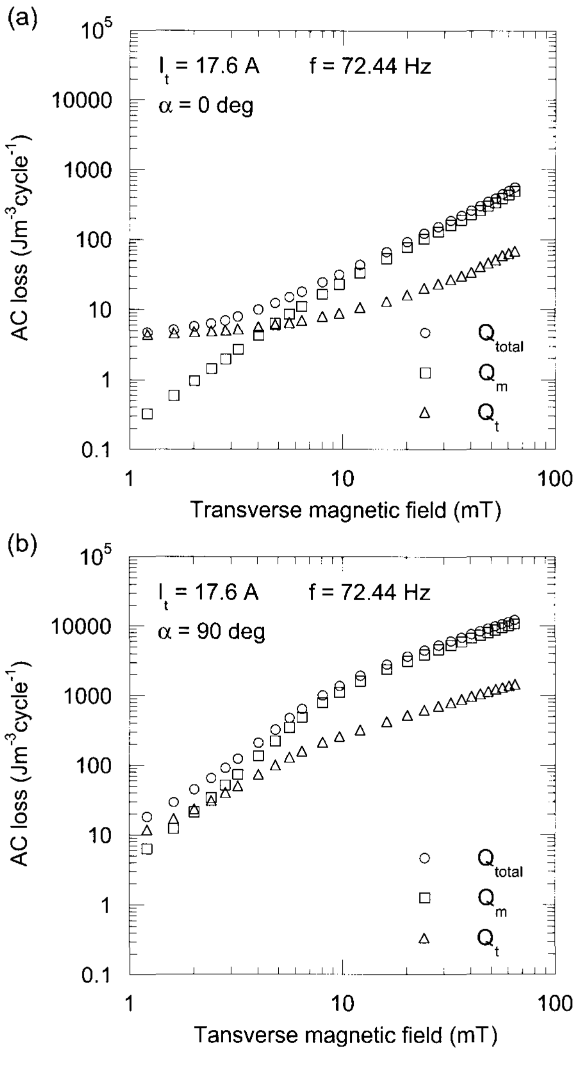

Fig. 3. Measured magnetization loss Q_m, transport loss Q_t, and total loss Q_{total} in a twist BSCCO multifilamentary tape: (a) in parallel magnetic field and (b) in perpendicular magnetic field.

the temporal evolution of current / magnetic flux distribution inside the superconductor calculated numerically using the finite element method. In our model, superconducting property is given by the power law *E-J* characteristic [12],

$$E = E_c \left(\frac{J}{J_c} \right)^n , \qquad (4)$$

where E_c = 1×10^{-4} V/m. The equivalent conductivity of superconductor σ_{sc} is derived as

$$\sigma_{sc} = \frac{J}{E} = \left(\frac{J_c^n}{E_c}\right) J^{1-n}. \tag{5}$$

In case of multifilamentary Bi-2223 superconductors, their filamentary region where superconducting filaments are embedded in the normal metal matrix is treated as a continuum mixture of superconductor and normal metal. The equivalent conductivity tangential to the filament, σ_f,

TABLE III.
SPECIFICATIONS OF Y-123 FILM CONDUCTOR FOR AC LOSS MEASUREMENTS

Conductor width	5 mm
Thickness of YBCO film	0.3 m
Thickness of sapphire substrate	0.53 mm
Critical current	42.8 A
n value	43

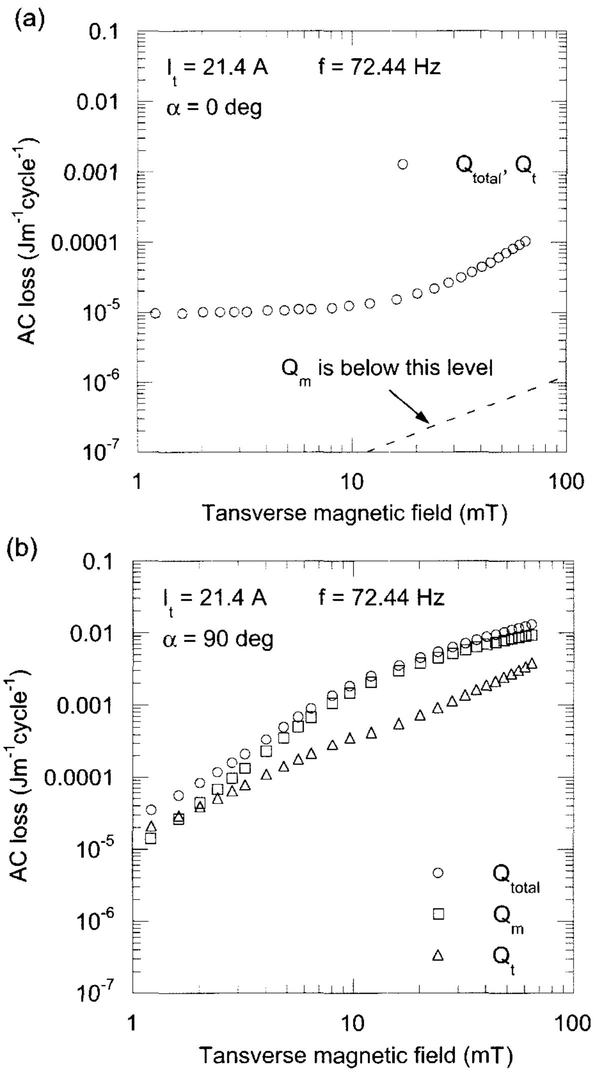

Fig. 4. Measured magnetization loss Q_m, transport loss Q_t, and total loss Q_{total} in an YBCO film conductor: (a) in parallel magnetic field and (b) in perpendicular magnetic field.

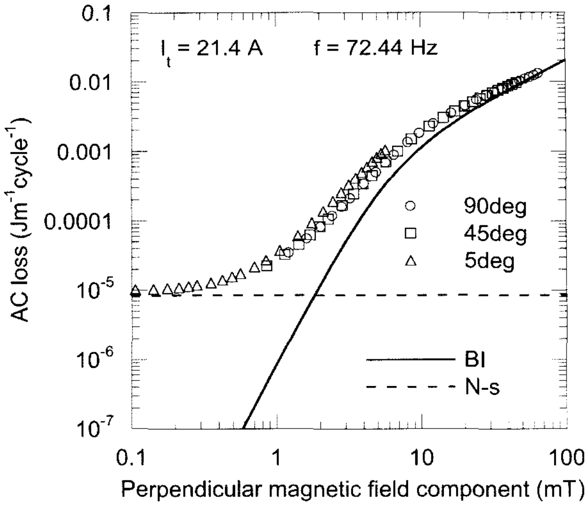

Fig. 5. Total loss in an YBCO film conductor versus perpendicular magnetic field component.

can be given as the average of the σ_{sc} and the σ_m weighted by the cross sections of the superconductor and the normal metal matrix, where the σ_m is the matrix conductivity. The equivalent conductivity perpendicular to the filaments is denoted by $\sigma_\perp$. Using σ_f, $\sigma_\perp$, and a filament direction vector $\boldsymbol{v}$ (v_x, v_y, v_z), the anisotropic Ohm's law with tensor equivalent conductivity is given as

$$\begin{pmatrix} J_x \\ J_y \\ J_z \end{pmatrix} = \begin{pmatrix} v_x^2(\sigma_f-\sigma_\perp)+\sigma_\perp & v_xv_y(\sigma_f-\sigma_\perp) & v_xv_z(\sigma_f-\sigma_\perp) \\ v_xv_y(\sigma_f-\sigma_\perp) & v_y^2(\sigma_f-\sigma_\perp)+\sigma_\perp & v_yv_z(\sigma_f-\sigma_\perp) \\ v_xv_z(\sigma_f-\sigma_\perp) & v_yv_z(\sigma_f-\sigma_\perp) & v_z^2(\sigma_f-\sigma_\perp)+\sigma_\perp \end{pmatrix} \begin{pmatrix} E_x \\ E_y \\ E_z \end{pmatrix}. \tag{6}$$

This anisotropic Ohm's law is used as the constitutive equation to solve the Maxwell's equations to calculate the electromagnetic field numerically [13]. The trace of a filament is spiral whose trajectory is shown in Fig. 6. Then, $\boldsymbol{v}$(v_x, v_y, v_z) is defined as

$$\boldsymbol{v} = \frac{1}{v'} \begin{pmatrix} \sin\phi\sin\theta \\ -a\sin\phi\cos\theta \\ \cos\phi \end{pmatrix}, \tag{7}$$

$$v' = \sqrt{(\sin\phi\sin\theta)^2 + (-a\sin\phi\cos\theta)^2 + (\cos\phi)^2}, \tag{8}$$

$$\phi = \tan^{-1}(2\pi r/l_p), \tag{9}$$

$$r = \sqrt{x^2 + (y/a)^2}, \tag{10}$$

where $\theta = \tan^{-1}(y/(ax))$ for $x \geq 0$, a is the ratio of the y to the x-axes of the tape, and l_p is the twist pitch.

In case of coated conductors, a simple scalar expression of Ohm's law can be used as the constitutive equation.

The author's code is formulated with the current vector potential $\boldsymbol{T}$ and magnetic scalar potential Ω,

$$\boldsymbol{J} = \nabla \times \boldsymbol{T}\ , \tag{11}$$

$$\boldsymbol{H} = \boldsymbol{H}_0 + \boldsymbol{T} - \nabla\Omega\ . \tag{12}$$

3.2. Numerical results

3.2.1. Numerical results for twisted Bi-2223 multifilamentary tape [13]

The current distribution in untwisted and twisted multifilamentary Bi-2223 tapes carrying AC transport current in an AC parallel transverse magnetic field were calculated, where $I_t/I_c = 0.7$, $B_m = 50$ mT, and $f = 50$ Hz. Specifications of tapes are listed in Table IV. An asymmetric current distribution is observed in the untwisted tape in Fig. 7(a), while the current distribution was symmetric in the twisted tape as shown in Fig. 7(b). This is an effect of twisting to reduce the AC loss.

3.2.2. Numerical results for rectangular superconductor

The current distribution in rectangular superconductor simulating coated conductors was calculated, when it was exposed to the perpendicular transverse magnetic field. Specifications of the superconductor are listed in Table V. The aspect ratio was reduced to 100 to suppress the number of elements. Fig. 8 shows the temporal evolution of the current distribution. In Fig. 9, the calculated magnetization loss as well as an analytical value given by Brandt and Indenbom [10] is plotted against the magnetic field. The numerical values almost agree with the analytical plot.

TABLE IV.
SPECIFICATIONS OF TWISTED BI-2223 MULTIFILAMENTARY TAPE FOR ANALYSIS

Tape width	4.0 mm
Tape thickness	0.25 mm
Twist pitch	20 mm
Critical current density	3.0×10^8 A/m^2
Transverse resistivity	3.0×10^{-7} Ωm

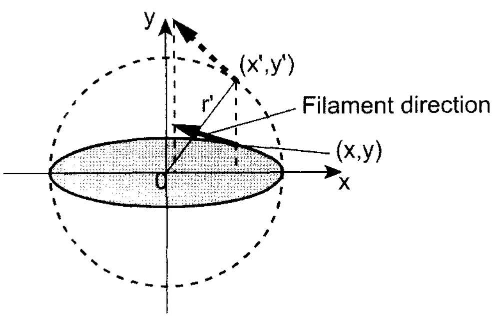

Fig. 6. Filament trajectory.

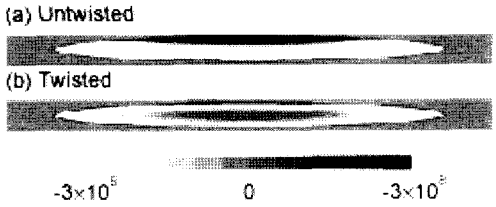

Fig. 7. Current distribution in cross section of BSCCO tapes carrying AC transport current in AC parallel transverse magnetic field: (a) untwisted tape and (b) twisted tape

TABLE V.
SPECIFICATIONS OF RECTANGULAR SUPERCONDUCTOR FOR ANALYSIS

Conductor width	10.0 mm
Conductor thickness	0.1 mm
Critical current density	3.0×10^8 A/m^2

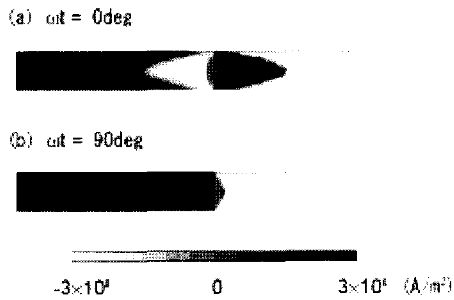

Fig. 8. Current distribution in cross section of rectangular superconductor.

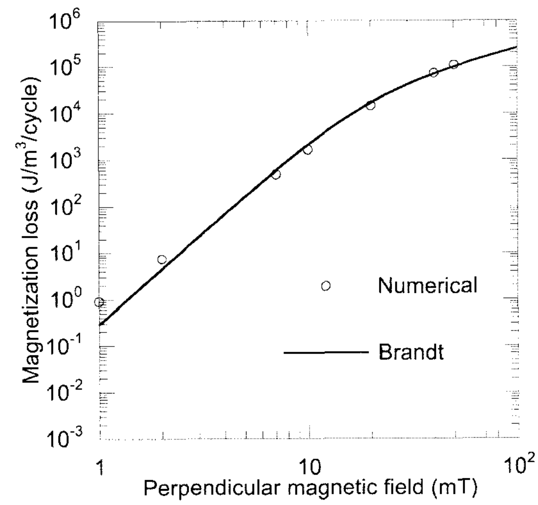

Fig. 9. Magnetization loss of rectangular superconductor in perpendicular magnetic field.

4. SUMMARY

The experimental and numerical approaches for AC loss estimation in high Tc superconductors were reviewed. The AC loss characteristics of high Tc superconductors can be revealed through these two approaches for their practical applications to AC electrical devices.

In this article, we focused on AC loss estimation of single conductor. In principle, AC loss characteristics of windings can be evaluated by integration of the AC loss characteristics of single conductor.

ACKNOWLEDGMENT

AC loss measurements of both Bi-2223 tape & Y-123 film conductor and numerical calculations of Bi-2223 tapes were supported in part by a grand for an international cooperative research in DAPAS program by the CAST, a part of the 21st Century Frontier R&D Program funded by the Ministry of Science and Technology, Republic of Korea. The author acknowledges the members of the author's group for their assistance in preparing this article.

REFERENCES

[1] Z. Jiang and N. Amemiya, "An experimental method for total AC loss measurement of high Tc superconductors," *Supercond. Sci. Technol.,* vol. 17, pp.371-379, 2004.

[2] J. J. Rabbers, B. ten Haken, and H. H. J. ten Kate, "Advanced ac loss measurement methods for high-temperature superconducting tapes,"*Review of scientific instruments*, vol. 72, pp. 2365-2373, 2001.

[3] J. Ogawa, Y. Yanagihara, Y. Yamato, and O. Tsukamoto, "Measurements of total AC losses in HTS short sample wires by electric and calorimetric methods," *Adv. Cryogenic Eng.*, submitted for publication.

[4] S. Fukui, Y. Kitoh, T. Numata, O. Tsukamoto, J. Fujikami and K. Hayashi, "Transport current AC losses of high-Tc superconducting tapes exposed to AC magnetic field," *Adv. Cryogenic Eng.*, vol.44, pp.723-730, 1998.

[5] M. Iwakuma, M. Nanri, M. Fukui, Y.Fukuda, K. Kajikawa and K. Funaki,"Theoretical investigation on the detection ratio of the magnetization in superconducting wires by a saddle-shaped pick-up coil," *Supercond. Sci. Technol.*, vol.16, pp.545-556, 2003.

[6] Z. Jiang, N. Amemiya, T. Nishioka, and S.-S.Oh,"AC loss measurements of twisted and untwisted BSCCO multifilamentary tapes," *Cryogenics*, submitted for publication.

[7] Z. Jiang, N. Amemiya, N. Ayai and K. Hayashi, "AC loss measurements of twisted and non-twisted BSCCO tapes in transverse magnetic field with various directions," *IEEE Transactions on Applied Superconductivity*, vol. 13, No. 2, pp. 3557-3560, 2003.

[8] N. Amemiya, Z.Jiang and T. Nishioka, "Comparison between AC loss characteristics of YBCO coated conductors and BSCCO multifilamentary tapes," *ASC-2004,* abstract submitted for presentation.

[9] N. Amemiya, T. Nishioka, Z. Jiang and K. Yasuda, "Influence of film width and magnetic field orientation on AC loss in YBCO thin film," *Supercond. Sci. Technol.*, vol. 17, pp. 485-492, 2004.

[10] N. Amemiya, S. Murasawa, N. Banno and K. Miyamoto, "Numerical modelings of superconducting wires for AC loss calculations," *Physica C*, vol. 310, pp. 16-29, 1998.

[11] N. Amemiya, N. Enomoto and S. Shirai, " FEM Analysis of AC Loss in Twisted Bi-2223 Multifilamentary Tapes Carrying AC Transport Current in AC Transverse Magnetic Field with Arbitrary Orientation," *IEEE Transactions on Applied Superconductivity*, submitted for publication.

[12] E. H. Brandt and M. Indenbom, "Type-II-supenconductor strip with current in a perpendicular magnetic field," *Physical Review B*, vol. 48, pp. 12893-12906, 1993.

[13] W. T. Norris, "Calculation of hysteresis losses in hard superconductors carrying ac:isolated conductors and edges of thin sheets," *J. Phys. D: Appl. Phys.*, vol.3, pp.489-507, 1970.